Journal of Sedimentary Research

Journal of Sedimentary Research, 2010, v. 80, 288–299
Research Article
DOI: 10.2110/jsr.2010.029

COMPOSITION AND PROVENANCE HISTORY OF LATE CENOZOIC SEDIMENTS IN SOUTHEASTERN BOLIVIA: IMPLICATIONS FOR CHACO FORELAND BASIN EVOLUTION AND ANDEAN UPLIFT

CAROLA HULKA* AND CHRISTOPH HEUBECK
Freie Universität Berlin, Department of Geological Sciences, Malteserstraße 74-100, 12249 Berlin, Germany
e-mail: cheubeck@zedat.fu-berlin.de

ABSTRACT: The Chaco foreland basin marks the eastern edge of the Andean orogenic system and contains up to 7.5 km of mostly nonmarine siliciclastics, thus providing an opportunity to study the detrital record of late Cenozoic Andean geodynamics and paleogeography. Sandstones from the southern Bolivian Chaco foreland basin testify to variable contributions from the craton and the Andean foreland fold-and-thrust belt in the context of an eastward-advancing orogen. Sandstone and conglomerate petrography of the Oligocene to Recent strata exposed in the Chaco Basin show an overall trend towards reduced mineralogical maturity, corresponding to diminishing transport distance, increasing topographic gradient and changing depositional environment from arid continental plain (Oligocene to middle Miocene Petaca sandstone) through marginal marine (middle Miocene to late Miocene Yecua sandstone) and braided fluvial settings (late Miocene Tariquia sandstone) to semihumid alluvial-fan environments (late Miocene to Recent Guandacay and Emborozú formations).

Paleocurrent patterns of pre-tectonic sediments record westward transport. The late Miocene transitional-marine Yecua Formation sediments show a complex shoreline-related pattern. Syntectonic strata (Tariquia, Guandacay, and Emborozú formations) filling the foreland basin indicate dominant east-directed sediment transport from the advancing Andean orographic front. Because the Eastern Cordillera provided a drainage barrier to Altiplano erosion, sandstones of the Chaco Basin do not directly record Andean volcanism or Altiplano uplift; however, climatic inferences from changing facies and petrographic composition suggest major uplift and formation of orographic barriers between 14 and 7 Ma.

INTRODUCTION

Sedimentary facies analysis and petrographic, geochemical, and geomorphologic studies have led to a good understanding of the climatic, transport-related, and tectonic components which jointly control the relative abundance of detrital components in sedimentary basins (e.g., Blatt 1967; Dickinson and Suczek 1979; Suttner and Basu 1981; Mack 1984; Bilodeau and Keith 1986; Johnsson 1990; Johnsson et al. 1991). Unraveling the dynamic coupling of these controls in the evolution of mountain belts has been the subject of numerous field and modeling studies (e.g., Willett 1999; Whipple and Meade 2006). Because deciphering the principal mechanisms governing spatio-temporal patterns of vertical and lateral growth of structurally complex orogens is crucial to their understanding, a close reading of the archives of erosional denudation and timing of deformation in adjacent foreland basins through provenance analysis and age dating usually contributes to that objective.

Due to generally good exposure and numerous datable volcanic ash units in the thick foreland strata of southern Bolivia (Uba et al. 2007; Uba et al. 2009), the Subandean fold-and-thrust belt and the adjacent Chaco foreland basin provide a favorable setting to study the interaction between tectonics and climate in a mountain belt and implications for Andean uplift (Fig. 1). To date, however, no petrographic information contributes to the controversial discussion on timing of deformation in the Subandean fold-and-thrust belt and Andean uplift (e.g., Baby et al. 1992; Gubbels et al. 1993; Dunn et al. 1995; Coudert et al. 1995; Moretti et al. 1996; Kley et al. 1997; Echavarria et al. 2003; Uba et al. 2006; Ege et al. 2007; Uba et al. 2007; Barnes et al. 2008; Uba et al. 2009).

Ege (2004), Ege et al. (2007), and Barnes et al. (2008) documented a rapid increase in exhumation rates in the Interandean and Subandean zones between 12 and 5 Ma using apatite fission-track thermochronology. Their interpretation is supported by recent geochronologic data that show the arrival of thrusting in the Subandean zone at 12.4 Ma and the subsequent rapid propagation toward the foreland unit at ca. 6 Ma (Uba et al. 2009). The fourfold increase in sediment accumulation rates in the region between 8 and 6 Ma (Uba et al. 2007) suggest that surface uplift probably had occurred before or during this time. In order to explain the large variations in foreland sedimentation rates in the central Andes, changes in tectonic rates have been invoked by Echavarria et al. (2003), whereas Uba et al. (2007) suggested climatic forcing related to the South American monsoon. Mulch et al. (2009) and Strecker et al. (2006) used Sr-, C-, and O-isotopic data to document climatic variability and the onset of the South American monsoon at ca. 8.5 Ma.

To close the gap between these studies, we examined the composition of Oligocene–Recent siliciclastic strata from the Chaco foreland basin, Bolivia, which were derived from sedimentary, metamorphic, and magmatic sources under arid to semihumid conditions (Fig. 1). The Chaco Basin contains up to 7.5 km of pretectonic and syntectonic sediment (Gubbels et al. 1993; Dunn et al. 1995; Moretti et al. 1996; Uba et al. 2005). Strata in its western part have become involved in the actively prograding deformation front of the Andes (Sempere et al. 1990; Dunn et

* Present Address: Zwerggasse 1, 1020 Wien, Austria

 1527-1404/10/080-288/$03.00

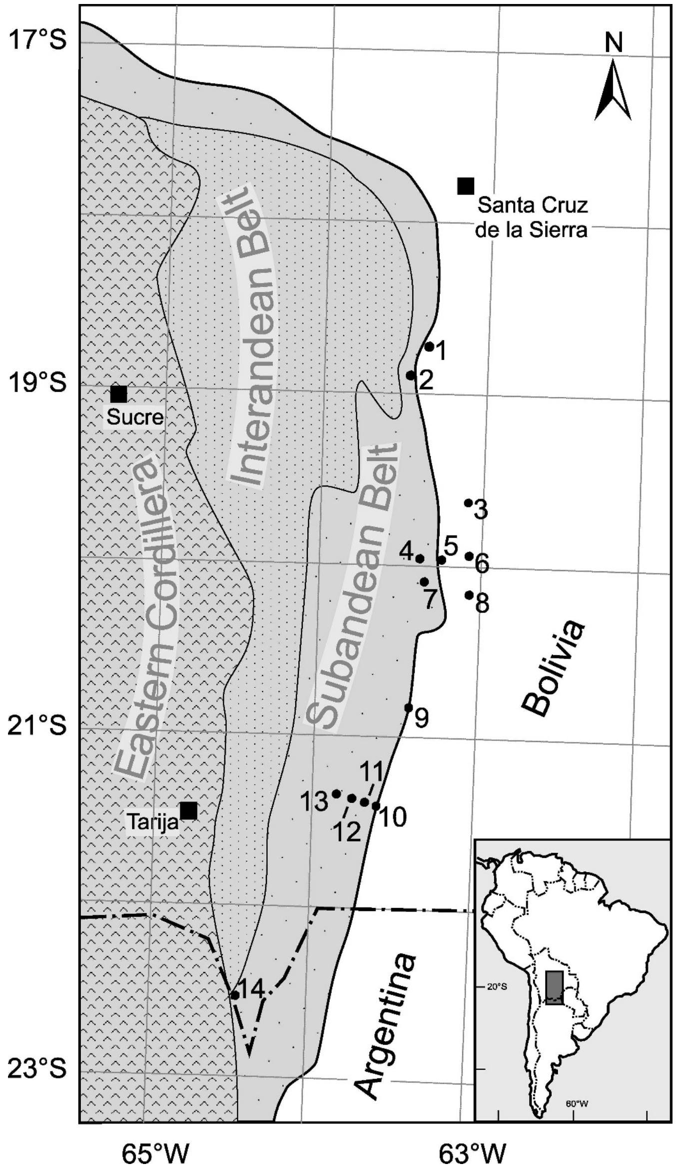

FIG. 1.—Tectonic sketch map of the Bolivian Chaco Basin (modified after Suárez Soruco, 2000), showing measured and sampled sections along the western margin of the Subandean belt. Locations: 1, Abapó; 2, Tatarenda; 3, Pirití; 4, Camiri; 5, Choretí; 6, San Antonio; 7, Cambeití; 8, Ivoca; 9, Macharetí; 10, Villamontes; 11, Salvación; 12, Zapaterimbia; 13, Rancho Nuevo; 14, Emborozú.

al. 1995; Moretti et al. 1996; Kley 1996); this fold-and-thrust zone is known as the Subandean Belt (or Zone) and represents the easternmost deformed structural domain of the central Andes. The late Cenozoic Chaco basin, consisting of dominant sandstone, mudstone, and conglomerate, as well as minor shell hash coquinas, evaporites, and volcanic tuffs, therefore provides a detrital record of foreland-basin dynamics and central Andean uplift and eastward propagation, gradually overriding the retroarc foreland basin and incorporating it into the fold-and-thrust belt.

Previous studies in this part of the Andes have documented the sedimentary and structural architecture, subsidence history, and basin development (Gubbels et al. 1993; Coudert et al. 1995; Moretti et al. 1996; Jordan et al. 1997; Echavarria et al. 2003; Uba et al. 2005; Uba et al. 2007; Uba et al. 2009). However, the provenance history of the basin fill, its tectonic and climatic controls, and the evolution of the Chaco foreland basin and the Subandean zone remain poorly understood.

Here, we present and interpret new data from a petrographic study of the late Cenozoic Chaco Basin foreland of southeastern Bolivia. The study area extends from the city of Santa Cruz in the north to the Argentine border in the south, mostly utilizing outcrop sections along the easternmost anticlines of the Subandean zone (Fig. 1). Our study aims to shed light on the sediment source areas and structural controls on foreland-basin development and the timing of the Andean uplift. We address in particular questions of variations in basin geometry, climatic influence, and the timing of orogenic processes in the central Andes.

GEOLOGIC SETTING AND LATE CENOZOIC STRATIGRAPHY

Tectonic History

Uplift and exhumation of the central Andes started in the central Eastern Cordillera in the late Eocene (ca. 42 Ma) and propagated since the Oligocene (ca. 32 to 20 Ma) as a result of upper-basement shortening to the eastern part of the Eastern Cordillera (Horton et al. 2002; Ege et al. 2007; Barnes et al. 2008). The exhumation front was situated in the central Interandean belt in the early Miocene (ca. 18 Ma) and reached the western Subandean zone in the late Miocene (ca. 12 to 8 Ma) (Gubbels et al. 1993; Barke and Lamb 2006; Ege et al. 2007; Uba et al. 2007; Uba et al. 2009). Moretti et al. (1996) and Uba et al. (2009) concluded that the central Subandean zone was probably not affected by deformation until 6 Ma.

The Subandean zone and the Chaco foreland basin developed as a result of subduction of the oceanic Nazca plate below the South American plate and the simultaneous westward underthrusting of the Brazilian Shield under the growing Andes, triggering eastward migration of thrusting (Sempere et al. 1990; Uba et al. 2006; Uba et al. 2009). The Subandean zone is characterized by thin-skinned, in-sequence and partially blind thrusting and folding (Baby et al. 1992; Dunn et al. 1995; Echavarria et al. 2003; Uba et al. 2006). Based on new thermochronologic data, Ege (2004) and Barnes et al. (2008) showed that the Subandean zone experienced rapid cooling during the late Miocene. Recently, Uba et al. (2009) used U-Pb ages of volcanic tuffs to document the timing and geometry of deformation in the zone.

Allmendinger et al. (1997) documented voluminous ignimbrites of late Miocene and Pliocene age (3–2 Ma) from the southern Altiplano and Puna plateaus and its margins. Ignimbrites 8–6.5 Ma old are also known from the eastern Altiplano and the western part of the Eastern Cordillera (Allmendinger et al. 1997). Coira et al. (1993) described backarc stratovolcano–caldera complexes during that time.

Regional Stratigraphy

The late Cenozoic lithostratigraphy of the Chaco basin fill is conventionally subdivided into five formations: the Petaca, Yecua, Tariquia, Guandacay, and Emborozú formations (Marshall and Sempere 1991; Gubbels et al. 1993; Fig. 2). The up to 200-m-thick Petaca Formation probably overlies a low-relief Mesozoic land surface with unconformable contact. It consists of calcrete, reworked pedogenic clasts, and redbed sandstone and mudstone (Fig. 3A; Uba et al. 2005). This unit represents extensive pedogenesis under an arid to semiarid climate, modified by ephemeral braided streams (Uba et al. 2005; Uba et al. 2006). The age of the Petaca Formation is poorly constrained. A Deseadean notohippid (an extinct family of notoungulate mammals used in South American land-mammal stratigraphy) found near the base of the Petaca Formation indicates a late Oligocene–early Miocene age (~ 27 Ma; Marshall and Sempere 1991; Marshall et al. 1993). Uba et al. (2007) documented an isotopic age of 12.4 Ma near the base of the overlying Yecua Formation.

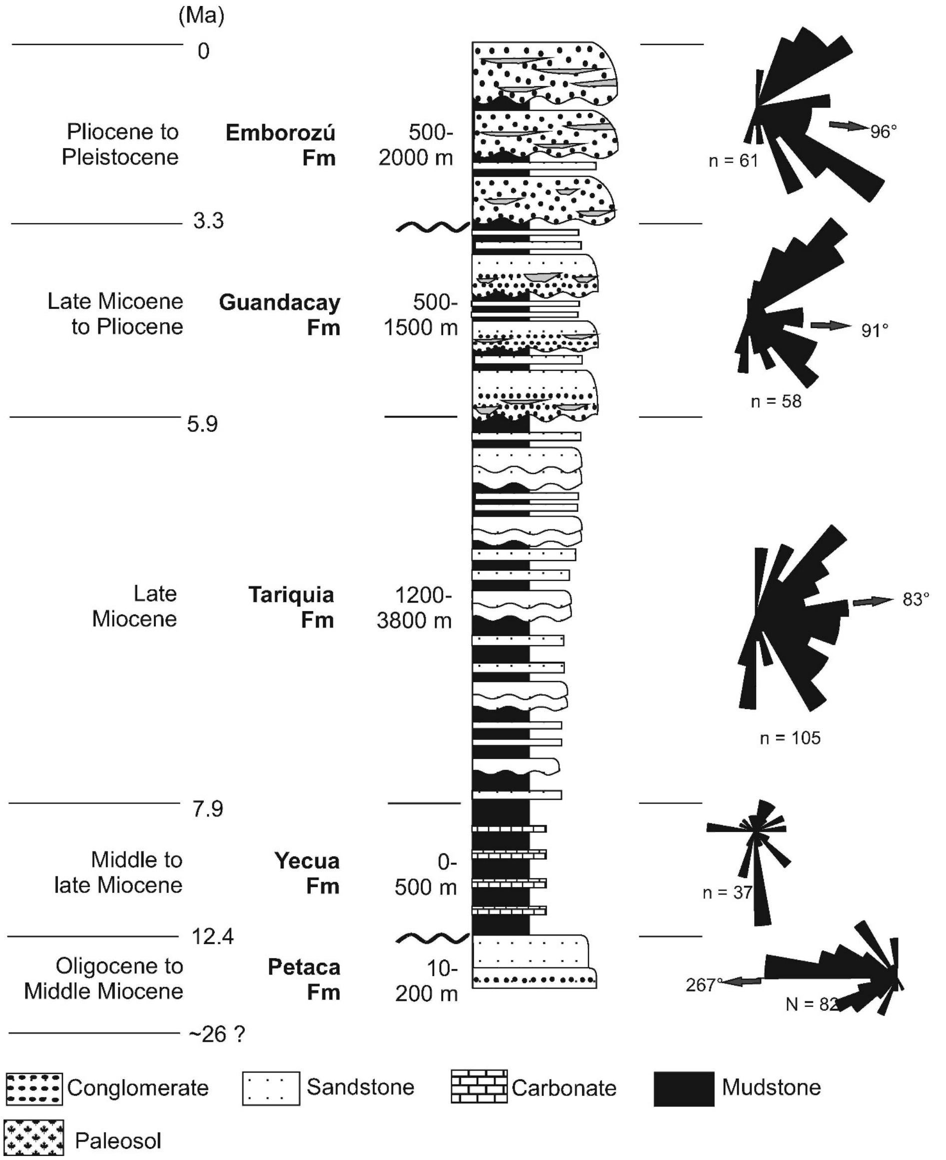

FIG. 2.—Schematic time-stratigraphic and lithostratigraphic column of the Chaco Basin strata in Subandean outcrops (compiled from the sections in Fig. 1 and from Uba et al. 2005), also showing paleocurrent rose plots (Hulka 2005). Note the long time span condensed in the thin continental-interior-facies Petaca Formation and the comparatively short time spans represented by the thick foreland-basin-fill Tariquia, Guandacay, and Emborozú formations.

The up to 500-m-thick Yecua Formation overlies the Petaca Formation unconformably. It consists of varicolored mudstone, calcareous and quartzitic sandstone, thin shell-hash coquinas, and minor ooid limestone representing restricted marginal marine, coastal floodplain, lacustrine, tidal, and medium-energy sandy shoreline environments (Fig. 3B; Uba et al. 2005; Hulka et al. 2006). Foraminifera indicate a restricted marginal-marine environment at 14–7 Ma (Hulka et al. 2006). U-Pb dating of a volcanic ash unit suggests the age of the Yecua Formation to be 12.4–7.9 Ma (Uba et al. 2007; Uba et al. 2009).

The up to 3800-m-thick Tariquia Formation transitionally overlies the Yecua Formation and consists of thick sandstone with lenticular geometry and red mudstone representing anastomosing stream channels and floodplains in distal segments of megafans (Fig. 3C; Uba et al. 2005, 2006). Marshall and Sempere (1991) described fish fossils along the base of the Tariquia Formation of Chasicoan to Huayquerian age (8–6 Ma). Biostratigraphic data suggest that the base of the Tariquia Formation is approximately 7 Ma old (Hulka et al. 2006). Radiometric age data constrain the age of the Tariquia Formation strata to the ~ 7.9–5.9 Ma time interval (Uba et al. 2007).

The up to 1500-m-thick, sandstone-dominated Guandacay Formation shows a coarsening- and thickening-upward sequence in a braided-stream in a medial fluvial megafan environment including lenticular sandstone, gravel sheets, and thin subordinate mudstone (Fig. 3D; Uba et al. 2005; Uba et al. 2006). A local angular discontinuity of late Miocene age (~ 6 Ma) between the Tariquia Formation and the Guandacay Formation at the La Vertiente Fault in southern Bolivia is interpreted on reflection-seismic lines (Moretti et al. 1996; Uba et al. 2006; Uba et al. 2009). Uba et al. (2007) and Uba et al. (2009) documented a volcanic ash of age 5.9 Ma at the base of the Guandacay Formation. Marshall and Sempere (1991) described the skeleton of a notoungulate (an extinct order of hoofed mammals native to South America) near the base of the Guandacay Formation, suggesting a Chasicoan to Huayquerian age (> 5.3 Ma).

Lastly, the up to 2000-m-thick Emborozú Formation represents the youngest unit within the Chaco Basin fill. This formation consists predominantly of coarsening-up cobble and boulder conglomerate, subordinate sandstone, and sandy mudstone, representing alluvial-fan deposition in a proximal fluvial megafan. Moretti et al. (1996) dated a volcanic tuff within the Emborozú Formation at 3.3 Ma.

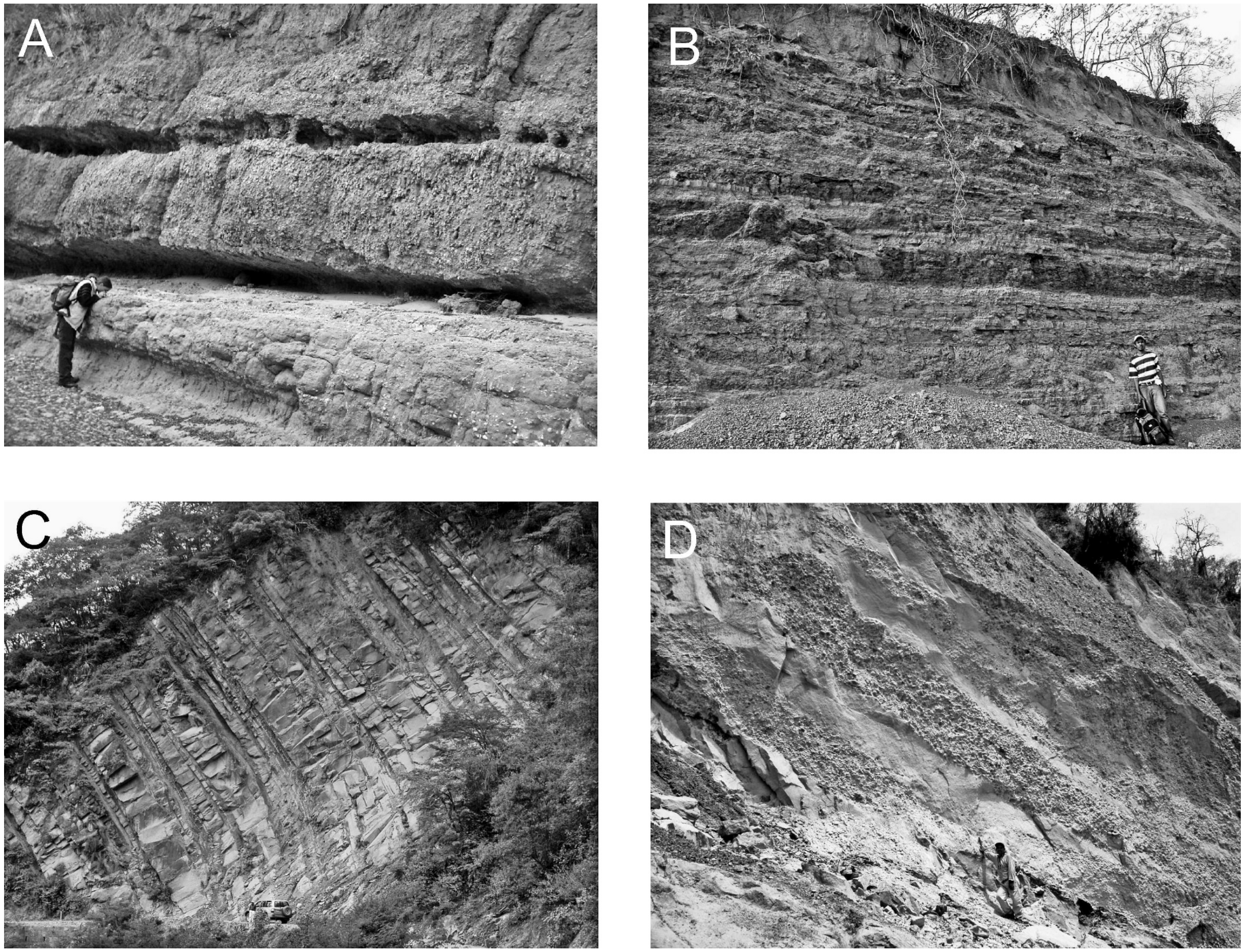

FIG. 3.—Outcrop photograph showing: **A)** sandstone and pedogenic conglomerate of the Petaca Fm., consisting of white calcrete and silcrete clasts, Ibuamirante section; **B)** interbedded thin-bedded sandstone and mudstone of the Yecua Fm, Abapo section; **C)** thick-bedded sandstone and thin-bedded mudstone of Tariquia Fm., Oquitas section; and **D)** Conglomerate and sandstone of Guandacay Fm., Emborozú section.

BASIN MARGIN TECTONICS

The geographic setting of the Chaco Basin allows the following geological regions to be potential contributors to the basin fill (Fig. 4): (1) the uplifted backarc region of the central Andes to the west, (2) the Brazilian Shield and Sierras Chiquitanas to the northeast, (3) the Izozog Arch to the east, (4) the Santa Barbara System to the south, and (5) the Amazon Basin to the north along depositional strike. Delivery of Subandean sedimentary and metasedimentary material from the west clearly dominates the recent basin fill (Horton et al. 2002; Uba et al. 2006).

Rocks of the Brazilian Shield, including high-grade granulites and low-grade greenschists, are exposed north and northeast of the Chaco Basin. The Sierras Chiquitanas, part of the southeastern margin of the Brazilian Shield, represent a mobile belt of Late Proterozoic to Cambrian metasediments (Fig. 4; Jones 1985). To the east, the strata of the Chaco Basin gradually pinch out against the Izozog arch. This region was probably exposed at the surface as early as the Carboniferous (Moretti et al. 1996) and represents a long-lived area of erosion or/and nondeposition. Using seismic and wireline-log data, Uba et al. (2006) suggested that the Izozog Arch comprises sedimentary strata of up to Devonian age.

During its entire history, the Chaco foreland basin was bordered to the west by the eastward-prograding front of the Subandean fold-and-thrust belt. This orogenic front presently recycles the basin fill by uplifting and deforming the western margin of the Chaco Basin. The Subandean zone exposes a thick sequence of Mesozoic and Paleozoic strata in anticlinal cores and thrust tips, mostly representing continental-interior depositional environments. Deformation in the central Subandean belt started ca. 6 Ma ago (late Miocene; Kley 1993; Echavarria et al. 2003; Uba et al. 2009), limiting its contribution to the Chaco Basin to the Tariquia Formation and the younger units. Ege et al. (2007) and Barnes et al. (2008) estimated about 6 km of post-Miocene erosion in this zone.

The Subandean fold-and-thrust belt is separated to the west by a major thrust from the adjacent narrow Interandean Belt, which presently exposes mostly Silurian–Devonian and minor Carboniferous sedimentary strata (Kley 1996; Müller et al. 2002). The thickness of formerly overlying, now-eroded strata is speculative but can be inferred from thermochronology in the following way (Ege et al. 2007): The Eastern Cordillera, west of the Interandean zone, was uplifted and eroded beginning in late Oligocene (Gubbels et al. 1993; Ege et al. 2007; Barnes et al. 2008) and therefore likely contributed to the Chaco basin fill since that time. It consists principally of Ordovician sandstones, which may exceed

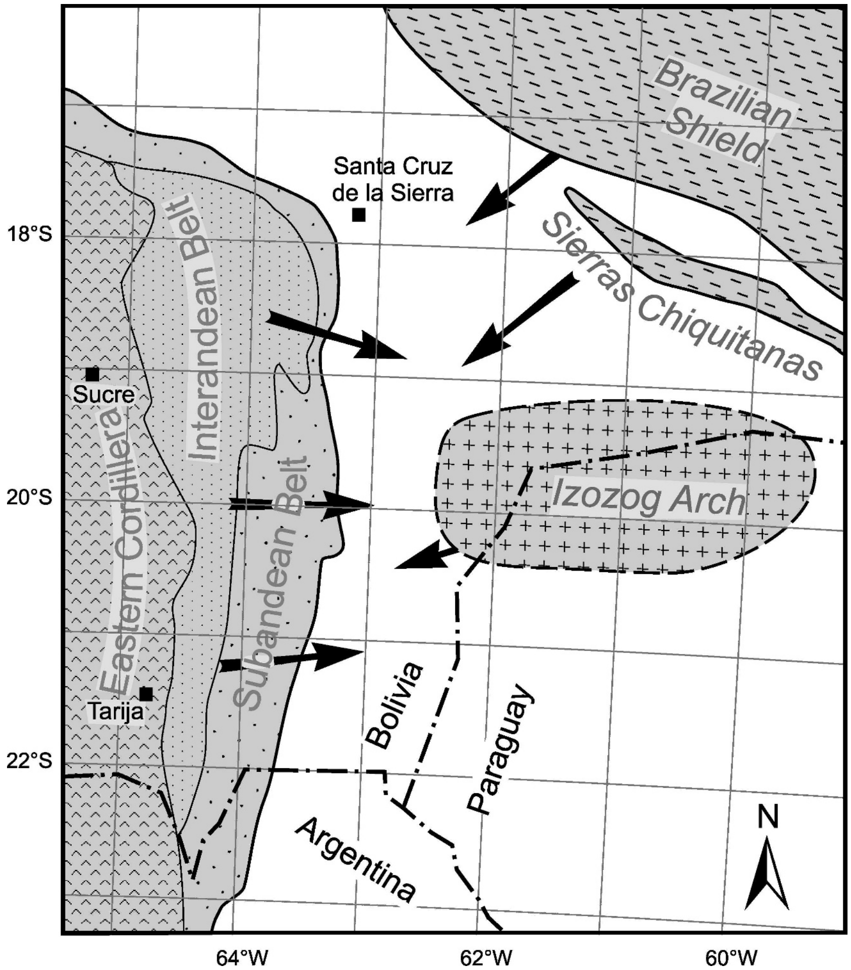

FIG. 4.—Potential provenance sources to the Chaco basin.

8 km in thickness (Erdtmann et al. 1995; Jacobshagen et al. 2002). Kley and Reinhardt (1994) concluded that these Ordovician rocks had been overlaid by 4–6 km of Paleozoic sediments which in turn had been unconformably overlain by up to 2.5 km of Cretaceous and Paleocene sandstone, mudstone, and subordinated lacustrine carbonate and pedogenically altered mudstone (Kley 1996; DeCelles and Horton 2003).

METHODS

We point-counted a total of 72 fresh sandstone samples from 14 locations of the Petaca, Yecua, Tariquia, Guandacay, and Emborozú formations (Fig. 1; Table 1), following the Gazzi-Dickinson method (Gazzi 1966; Dickinson 1970; Ingersoll et al. 1984). In each thin section, we counted 300 framework grains. Following the convention of Pettijohn (1975), we assigned grains < 0.03 mm to the matrix category. Provenance interpretation is aided by the measurements of 179 foresets of trough cross-beds and imbricate clasts of all formations for paleocurrent directions, mostly from fluvial environments (Fig. 2). Additional information came from visual inspection of conglomerate composition in the field.

Provenance studies are most effective by using a combination of several ternary diagrams rather than relying on a single diagram because combinations of specific end members discriminate between different grain properties. A standard combination, after Dickinson and Suczek (1979), includes Q-F-L, Qm-F-Lt, Qp-Lv-Ls, and Qm-P-K diagrams and subdivides the ternary diagram into different provenance fields related to tectonic regimes.

We combined our provenance analysis data with the U-Pb age data of late Cenozoic Subandean strata (Uba et al. 2007; Uba et al. 2009) to relate the spatio-temporal development of the Chaco foreland basin to Andean uplift. These datasets are augmented by results from fission-track thermochronology in the Eastern Cordillera and the Subandean zone (Ege et al. 2007; Barnes et al. 2008).

TABLE 1.—*Sample locations and number of sandstone samples used in modal analysis.*

Location	Emborozú Fm	Guandacay Fm	Tariquia Fm	Yecua Fm	Petaca Fm
Abapó	2	2			
Tatarenda		2	2	3	10
Pirití			1		2
Camiri			4		1
Choretí			1	1	4
San Antonio				2	3
Cambeití				1	1
Ivoca			2		2
Macharetí			2		2
Villamontes			2		2
Salvación			2		1
Zapaterimbia			3		1
Rancho Nuevo			3		1
Emborozú	4		3		
Σ	**6**	**4**	**25**	**7**	**30**

Sample locations are arranged north-to-south; see Fig. 1 for locations.

TABLE 2.—*Original sandstone point count data (n = 300) of 72 samples from the Bolivian Chaco Basin (Hulka, 2005).*

Section	Unit	*Sample Nr.*	Point Count Data Qm	Qp	P	K	Lv	Ls
Tatarenda	Guandacay	*370*	182	48	5	5	12	48
	Guandacay	*369*	189	32	10	5	15	49
	Tariquia	*365*	180	90	3	9	0	18
	Tariquia	*362*	112	102	20	20	0	46
	Yecua	*361*	296	2	2	0	0	0
	Yecua	*353*	289	7	2	0	0	2
	Yecua	*351*	292	4	4	0	0	0
	Petaca	*346*	290	0	7	0	0	3
	Petaca	*340*	260	22	18	0	0	0
	Petaca	*339*	265	25	5	0	0	5
	Petaca	*337*	261	21	16	0	0	2
	Petaca	*332*	270	20	5	0	0	5
	Petaca	*327*	254	25	17	4	0	0
	Petaca	*326*	251	20	27	2	0	0
	Petaca	*325*	263	24	8	5	0	0
	Petaca	*321*	251	31	7	11	0	0
	Petaca	*320*	252	20	11	17	0	0
Abapó	Emborozú	*154*	142	60	10	11	8	69
	Emborozú	*153*	100	50	49	32	30	39
	Guandacay	*160*	175	60	10	10	10	35
	Guandacay	*162*	180	60	7	6	10	37
Pirití	Tariquia	*100*	228	37	5	15	3	12
	Petaca	*95*	255	36	0	3	0	6
	Petaca	*90*	271	20	0	6	0	3
San Antonio	Yecua	*75*	243	36	6	12	0	3
	Yecua	*71*	259	20	2	15	0	4
	Petaca	*69*	257	20	5	7	0	11
	Petaca	*68*	241	30	13	15	0	1
	Petaca	*65*	259	20	10	2	0	9
Cambeití	Yecua	*60*	260	24	14	2	0	0
	Petaca	*58*	276	17	2	2	0	3
Choretí	Tariquia	*56*	235	48	3	5	0	9
	Yecua	*50*	240	32	7	14	1	6
	Petaca	*47*	256	20	10	14	0	0
	Petaca	*46*	250	26	3	15	0	6
	Petaca	*44*	252	24	12	12	0	0
	Petaca	*43*	262	17	12	9	0	0
Ivoca	Tariquia	*40*	252	35	2	3	1	7
	Tariquia	*39*	148	35	9	21	15	72
	Petaca	*36*	258	28	6	8	0	0
	Petaca	*33*	254	15	13	17	0	1
Camiri	Tariquia	*21*	183	74	8	5	8	22
	Tariquia	*20*	239	35	5	5	6	10
	Tariquia	*18*	186	53	10	11	10	30
	Tariquia	*14*	172	83	16	11	0	18
	Petaca	*1*	230	30	12	48	0	0
Machareti	Petaca	*103*	245	33	16	6	0	0
	Petaca	*136*	273	21	5	1	0	0
	Tariquia	*108*	247	23	12	1	1	16
	Tariquia	*120*	252	18	15	1	0	20
Angosto de Pilcomayo	Petaca	*314*	264	18	6	9	0	3
	Petaca	*329*	270	15	9	6	0	0
	Tariquia	*330*	261	11	9	10	0	9
	Tariquia	*334*	246	18	0	0	0	36
	Tariquia	*335*	234	21	9	0	0	36
Salvacion	Petaca	*402*	270	23	3	3	0	1
	Tariquia	*405*	234	45	4	0	0	17
	Tariquia	*411*	209	46	2	0	0	43
Zapaterimbia	Petaca	*803*	258	30	5	1	0	6
	Tariquia	*809*	268	18	4	0	0	10
	Tariquia	*813*	258	27	6	0	0	9

TABLE 2.—*Continued.*

Section	Unit	*Sample Nr.*	Point Count Data Qm	Qp	P	K	Lv	Ls
Rancho Nuevo	Petaca	*902*	258	27	12	3	0	0
	Tariquia	*903*	237	35	9	9	0	10
	Tariquia	*908*	244	30	6	1	0	19
	Tariquia	*920*	237	20	15	0	0	28
Emborozú	Tariquia	*E1*	234	9	12	0	0	45
Emborozú	Tariquia	*E2*	237	12	3	0	3	45
Emborozú	Tariquia	*E3*	222	24	0	0	0	54
Emborozú	Emborozú	*Emb4*	165	36	2	1	6	90
Emborozú	Emborozú	*Emb5*	172	40	10	14	0	64
Emborozú	Emborozú	*Emb6*	169	46	2	1	5	77
Emborozú	Emborozú	*Emb8*	164	43	9	2	22	60

Sample locations are arranged north-to-south; see Fig. 1 for locations.

Abbreviations: Qm = monocrystalline quartz, Qp = polycrystalline quartz, Fp = plagioclase, Fk = potassium feldspar, Lv = volcanic fragment, Ls = sedimentary fragment. Plutonic and metamorphic rock fragments were not observed.

RESULTS

Conglomerate Composition

Conglomerate stringers occur in the Petaca Formation, are absent from the Yecua (except for intrabasinal material) and Tariquia formations, and become dominant in the Guandacay and Emborozú formations. In the Petaca Formation, pebble conglomerates in laterally continuous beds up to 50 cm thick are composed nearly exclusively of calcrete and silcrete clasts and represent reworked, locally derived pedogenic horizons. Calcrete clasts are mostly moderately to well-rounded whereas the more resistant silcrete clasts are subangular.

Conglomerate clasts of the Guandacay Formation consist of oligomictic metaquartzites, which are generally matrix-supported and subangular to moderately rounded and occur in sheet-like units of maximum 10 m thickness. Individual clasts are usually 3 to 5 cm in diameter but can reach up to 10 cm. The dominant source consists of Ordovician and Mesozoic sandstones and quartzites from the central Andes (Uba et al. 2005). Conglomerates of the Emborozú Formation reach several meters thick and are generally clast-supported. Clasts are rounded to well rounded and show a median diameter of approximately 15 cm. Imbrication is common. Uba et al. (2005) identified Ordovician, Devonian, and Cretaceous sedimentary and metasedimentary rocks of the Subandean and Interandean belt as sources.

Grain Categories of Sandy Material and Diagenetic History

The following text briefly describes the major grain components of Petaca, Yecua, Tariquia, Guandacay, and Emborozú Formation sandstones. Results of thin-section point counts are listed in Table 2.

Quartz constitutes the highest proportion of grains in all sandstone samples. Monocrystalline quartz grains are typically rounded to very well rounded. More than 60% of the monocrystalline quartz grains show undulatory extinction; many quartz grains show inclusions (Fig. 5A). The proportion of polycrystalline quartz grains is generally lower than that of monocrystalline quartz (Fig. 5B). Domain boundaries may be straight or sutured. Fine- or coarse-grained chert as well as microcrystalline grains are rare to common. Feldspars are well preserved and angular to rounded. Corrosion by sericitization is common, particularly in coarse grains. Polysynthetic plagioclase twins are common (Fig. 5C). Potassic feldspars are untwinned and show Carlsbad twinning or distinctive Microcline twinning. Perthite intergrowth of plagioclase into potassic feldspar is common (Fig. 5D).

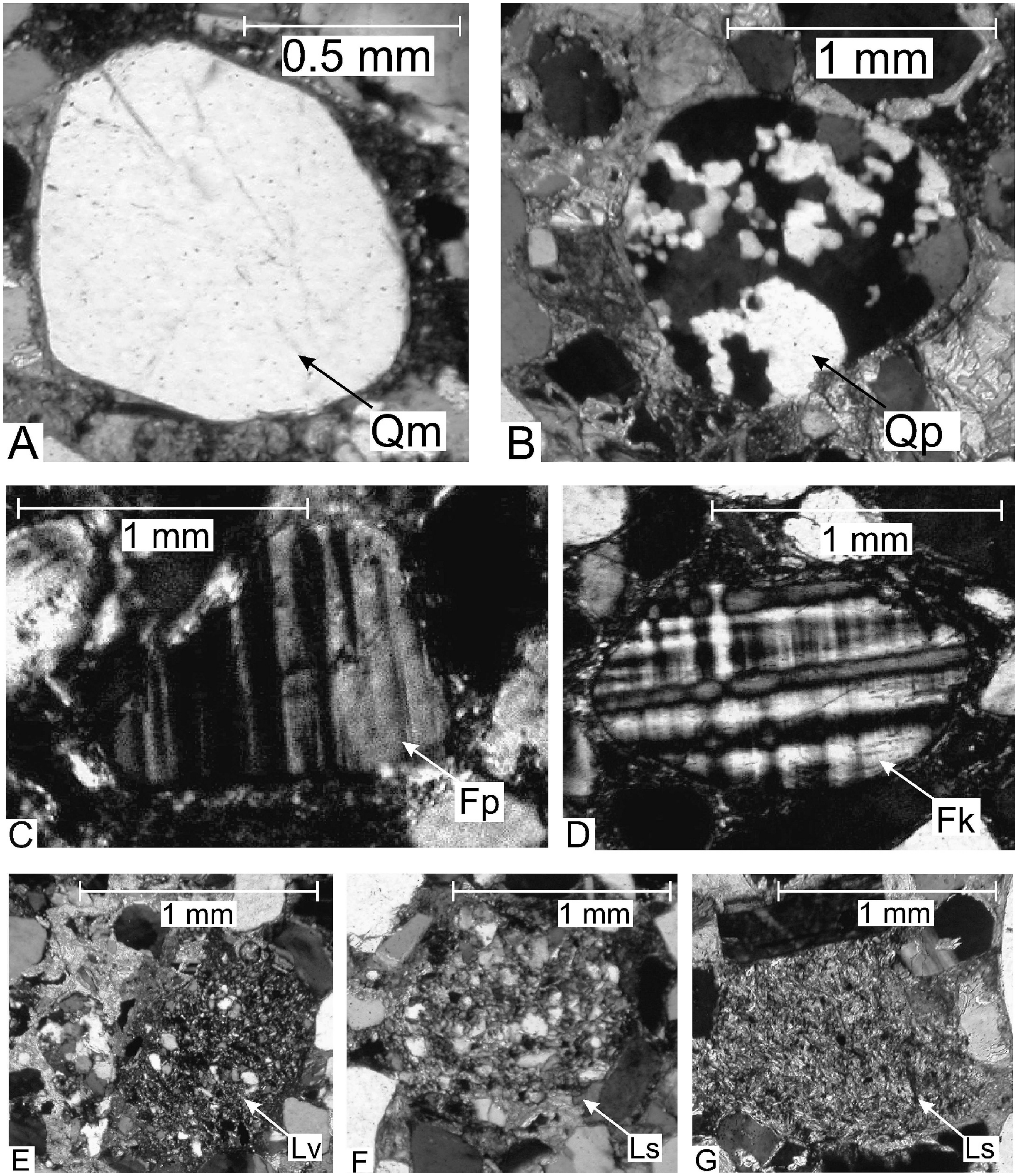

FIG. 5.—Thin-section photomicrographs of representative major framework grains from sandstones of the Chaco Basin. **A)** Monocrystalline quartz (Qm) of the Yecua Formation (San Antonio section); **B)** polycrystalline quartz (Qp) of the Yecua Formation (San Antonio section); **C)** plagioclase (Fp) of the Tariquia Formation (Camiri section); **D)** microcline (Fk) of the Tariquia Formation (Camiri section); **E)** lithic volcanic granular felsitic grain (Lv) of the Tariquia Formation (Camiri section); **F)** fine-grained sedimentary lithic fragments (Ls) of the Tariquia Formation (Camiri section); **G)** metasedimentary lithic fragments (Ls) of the Emborozú Formation (Abapó section). For locations, see Figure 1.

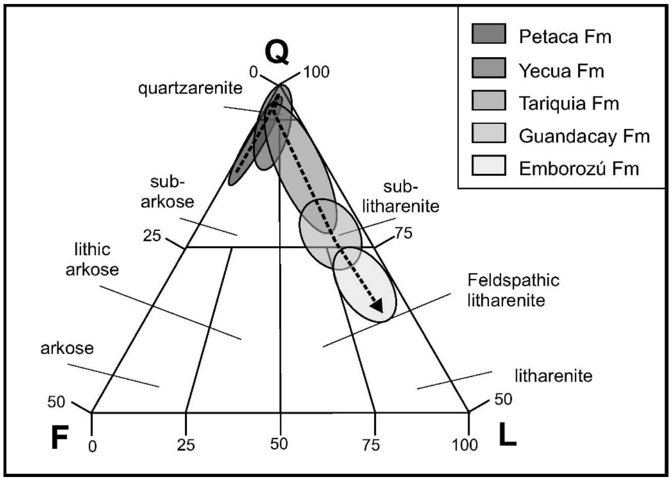

FIG. 6.—Sandstone clans of the five formations in the Chaco Basin in QFL diagrams showing stratigraphic-younging trend to more lithic composition. Definitions of grain populations follow Ingersoll et al. (1984). Subfields after Folk (1974).

Plutonic-sourced phaneritic lithic fragments are absent. Volcanic fragments contain microphenocrysts of quartz, biotite, and plagioclase in an opaque fine-grained groundmass (Fig. 5E). The few thin sections with substantial content of volcanic lithic fragments show mostly felsitic (dacite to rhyolite) grains with mainly anhedral microcrystalline quartz and feldspar, suggesting a felsic composition of its source rock (Critelli and Ingersoll 1995; Critelli et al. 2002). Lathwork, microlitic, and vitric grain types are absent. The occurrence of a balanced ratio of plagioclase to potassium feldspar and of quartz phenocrysts suggests an overall dacitic, rather than andesitic, contribution.

Sedimentary lithic grains include siliciclastic fragments and carbonate grains. The latter occur only in the Yecua Formation as intrabasinal ooid and reworked shell fragments and are therefore not included in the provenance calculations (e.g., Zuffa 1980; Critelli et al. 2007). Lithic grains consist largely of shale fragments, most of which include quartz and feldspar grains in a clayey groundmass (Fig. 5F, G). Sand-size micas are a minor constituent in the Tariquia, Guandacay, and Emborozú formations, with biotite more common than white mica. Opaque minerals and heavy minerals are rare.

The clayey matrix ranges between 5 and 10% in the Petaca Formation and Yecua Formation sandstones but is lower, ca. 5%, within the Tariquia, Guandacay, and Emborozú formations. The high interference colors of the clayey matrix suggest a high smectite content. Quartz and (commonly poikilotopic) calcite cement are common in the Petaca Formation, whereas chalcedonic cement is rare. Early calcite cement is widespread in the Yecua Formation; quartz cement is subordinate. In contrast, clay dominates the cement in the Tariquia, Guandacay, and Emborozú formations, with subordinate quartz cement. All cements appear early, postdating only the widespread formation of hematitic cutanes on grain surfaces. As a result, framework grains show in general little compaction, and pressure solution is generally minor to moderate, grain-to-grain contacts are tangential or straight, and detrital mica are slightly bent.

Sandstone Classification

Sandstones of the Petaca and Yecua formations are quartzarenites and quartz-rich subarkoses; only one sample of the Yecua Formation plots into the sublitharenite field (Fig. 6). The sandstone composition of the Tariquia Formation includes mainly sublitharenites to quartz-rich subarkoses. The four samples of the Guandacay Formation are from only two outcrops of the northern part of the Chaco Basin; they plot into the sublitharenite field. Because fresh outcrops of the Emborozú Formation sandstones are rare, we could study their composition in only six samples from two sections from the northern and the southern part of the basin, respectively. They are dominantly litharenites, except one sample of lithic–arkose composition. The quartz fraction is dominated by monocrystalline quartz. Plagioclase and alkali feldspar are approximately equally abundant, and the lithic fraction is dominated by polycrystalline quartz and (meta-)sedimentary lithic fragments.

Overall, Chaco Basin sediments are generally rich in quartz, with all samples exceeding 50% quartz; samples from the Petaca and the Yecua formations exceed 85% quartz. Sandstones of the Tariquia Formation are transitional, with quartz ranging between 95% and 60% (Fig. 7). Quartz content decreases in the Guandacay and the Emborozú formations to < 80%, mainly due to an increase of lithic fragments.

Paleocurrents

Paleocurrent indicators show that the major sediment sources were initially located to the east of the basin, later mostly to the west (Fig. 2).

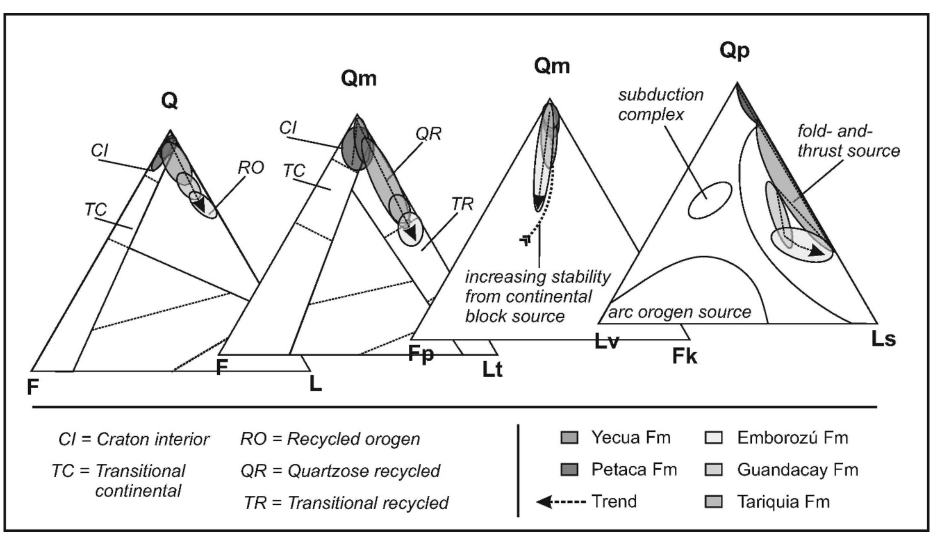

FIG. 7.—Tectonic provenance of Chaco basin sandstones. Provenance fields after Dickinson and Suczek (1979). Sandstones show a distinct trend towards more lithic character, reflecting increasing contributions of recycled sediment from the Andean fold-and-thrust belt. Volcanic contributions from the Andean arc are absent, reflecting the topographic barrier of the Eastern Cordillera. Abbreviations: CI = craton interior, TC = transitional continental, RO = recycled orogen, QR = quartzose recycled, TR = transitional recycled.

The paleoflow pattern in the Petaca Formation indicates a dominant westward transport direction whereas a weak bidirectional (N–S) transport direction appears prevalent in the polymodal directions from the Yecua Formation. Vectors of mean transport direction collected from imbricated clasts and fluvial cross beds in the Tariquia, Guandacay, and Emborozú formations consistently show a unimodal transport direction towards the east, with those of the Tariquia Formation exhibiting greater variability. These data demonstrate that fluvial–alluvial deposition since the late Miocene was dominated by Andean erosion and probably resembled the modern fluvial drainage pattern along the western margin of the basin. The high scattering of Tariquia paleocurrents is consistent with increased stream power and the beginning of fluvial megafan deposition as a result of transition from drier to more humid climate due to the onset of the South American monsoon (Uba et al. 2007), resulting in common avulsions and crevassing by anastomosing streams (Uba et al. 2005).

DISCUSSION

Provenance Analysis

Data on provenance and paleo-drainage show multiple sediment sources to the Chaco foreland between the late Oligocene to the present. Samples of the Petaca Formation plot within the craton-interior block of the tectonic-provenance diagram (Figs. 7, 8). Their position in the transport-sensitive Qm-F-Lt- and Qm-K-P-diagrams suggest a cratonic provenance. More than half of the point-counted samples fall close to the quartzose-recycled block (Fig. 8), indicating a high content of quartz resulting from a long transport distance, sedimentary recycling, or highly abrasive processes during transportation, such as in eolian environments or in high-bedload streams (Folk 1951; Cox and Lowe 1995). Indeed, all of these factors likely contributed to the composition of the Petaca Formation because Mesozoic bedrocks underlying the Petaca Formation include dominantly eolian quartzose sandstones of Cretaceous age (Gubbels et al. 1993); also, the low paleorelief of the Petaca Formation intensified sediment recycling from underlying material in the continental interior and likely caused long transport distances. The Qp-Lv-Ls-diagram (Fig. 8) confirms this interpretation with the dominance of polycrystalline quartz and minor (meta-) sedimentary lithic fragments, and by the absence of volcanic lithic fragments. The high percentage of craton-derived sediments and the west-directed paleocurrent pattern (Fig. 2) are consistent with the erosion of an eastern cratonic source, probably the Izozog Arch or the Brazilian Shield.

The extrabasinal components of Yecua sandstones (Fig. 8) show, except for an even lower feldspar and higher quartz content, a petrographic composition similar to that of sandstone from the Petaca Formation. They fall in the craton-interior block of Q-F-L- and Qm-F-Lt-diagrams. This trend is consistent with the weak N–S-directed paleocurrents, thus suggesting a source area to the northeast of the study area such as the Amazon region and the Brazilian shield. Facies analysis and fossils also suggest that the increased maturity of Yecua sandstone is due to reworking in shoreline systems (Hulka et al. 2006). Petrography points to a dominant cratonic source rock and a low contribution, if any, from Andean-derived recycled fold-and-thrust-belt material.

Tariquia Formation sandstones appear to indicate a mixed cratonic-interior and recycled-orogen provenance. In particular, the increasing proportion of Ls, dissimilar to the underlying formations, can be attributed to a recycled fold-and-thrust-belt provenance. This interpretation is consistent with the dominantly western paleocurrent pattern, which indicates the erosion of mostly sedimentary rocks. The compositional difference becomes best apparent in the high content of polycrystalline quartz and (meta-) sedimentary lithic fragments shown in the Qp-Lv-Ls-diagram (Fig. 8). The increased Q/F–ratio may indicate a high degree of chemical weathering, a long storage in soils, or extensive recycling of quartzose sandstones. All of these factors are consistent with the depositional setting and facies analysis of the Tariquia Formation (Uba et al. 2005).

The four samples of the Guandacay Formation are similar in composition and indicate a growing recycled-orogen and fold-and-thrust belt provenance (Fig. 8). Compared to the Tariquia Formation, quartz is reduced, compensated by a growing sedimentary lithic component. Magmatic sources, expressed by their feldspar contribution, do not yet appear in the provenance field.

The Emborozú Formation is largely conglomeratic. Interbedded sandstones may be limited in their information content due to their provenance from small, individual, well-defined drainage basins, which would explain the higher variability in the ternary diagrams. In addition, our data are limited to six samples from two sections. All of the ternary diagrams clearly indicate a recycled-orogen source (Fig. 8). One sample plots into the dissected-magmatic-arc source, possibly caused by a contribution by reworked tuffaceous components from a volcanic tuff bed just below the sample site. The reduced Qm content in the Qm-K-P-diagram may reflect the decreasing transport distance and better preservation of Lv and Qp grains. All of these observations fit well with the facies interpretation of the Emborozú Formation as having been deposited in an alluvial-fan environment.

Trends in Sandstone Composition

The sandstone composition of the Chaco Basin shows a consistent trend from mainly craton-interior continental source rock (Petaca Formation) to recycled-orogen sources of the Tariquia, Guandacay, and Emborozú formations (Fig. 7). The Yecua Formation shows a dominant craton-interior provenance but slightly reduced feldspar and increased lithic components, which we interpret as a beginning minor influence of recycled-orogen sources (Fig. 8). The Qm-K-P-diagram illustrates the gradually reduced continental provenance through increasing feldspar. The Petaca and the Yecua formations contain a high proportion of weathering-resistant Qp. The overlying formations, in contrast, show a decreasing contribution of Qp, compensated mostly by Ls, and clearly represent a fold-and-thrust-belt provenance. Volcanic lithic components remain low throughout.

Maturity

Textural and mineralogical maturity follow consistent trends in the Chaco foreland basin fill and collectively suggest that factors contributing to high maturity lose relative importance through time. Textural maturity of sandstone (Folk 1951) decreases stratigraphically upward throughout the section (Table 3). Indices of mineralogical maturity (Table 3) can identify weathering processes at the source or during transport because stable components are enriched relative to instable components while the ratio of polycrystalline to monocrystalline quartz considers the mechanical stability of sand grains. Mineralogical maturity in the Chaco Basin decreases upsection; only the Yecua value stands out, probably due to the high degree of reworking in shoreline systems.

Climatic Implications

The Oligocene climate in the study area (represented by deposits of the Petaca Formation) was likely arid or semiarid due to the occurrence of calcrete and silcrete paleosols and small eolian dune complexes. Uba et al. (2006) interpreted the dominance of reworked pedogenic clasts as indicating intrabasinal uplift and erosion of calcretes; however, we suggest that erosion during Petaca time could also have been driven by drier climate (Molnar and England 1990; Uba et al. 2005; Strecker et al. 2006; Mulch et al. 2009). Remobilized gypsum and ostracodes adapted to

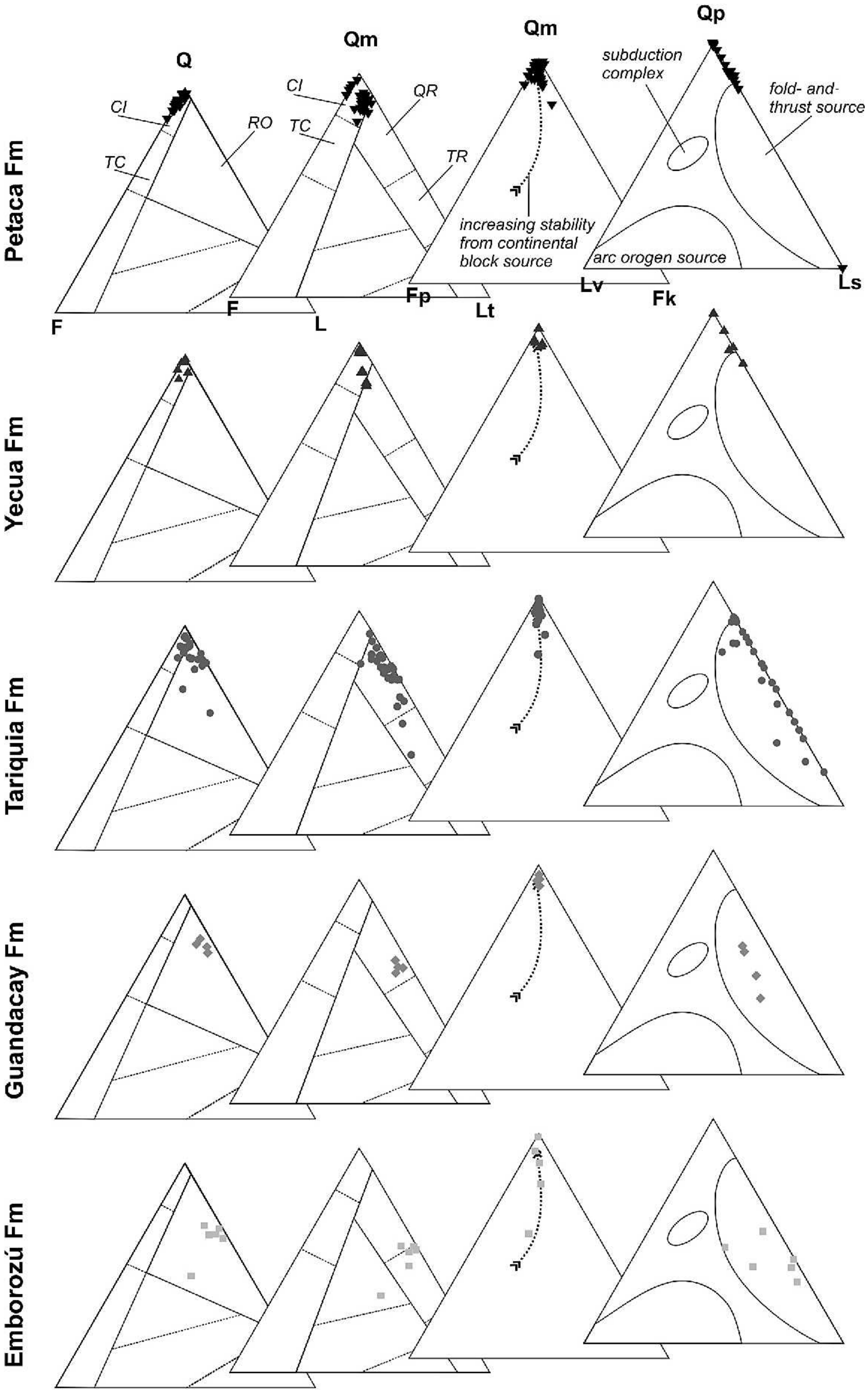

FIG. 8.—Detailed modal sandstone compositions, specific for each formation of the Chaco foreland basin. Counted (Qp, Qm, F, K, Lv, Ls) and recalculated parameters (Q, F, L, Lt) after Dickinson (1985) and Ingersoll et al. (1984). Tectonic-provenance fields as in Figure 7. Lithic sedimentary grains of the Tariquia Formation mark the beginning of Andean contribution to the basin fill. See text for discussion.

hypersalinity in sediments of the middle Miocene Yecua Formation also may indicate periodic semi-aridity (Hulka et al. 2006).

The increasing occurrence of root traces and thin coal seams and a concomitant decrease in abundance of calcretes, mudcracks, and rip-up clasts (Uba et al. 2005) as well as C-, O-, and Sr- isotopic data of Mulch et al. (2009) document a transition to increased humidity in latest Yecua time at ~ 8.5 Ma, contemporaneous with the onset of South American monsoonal climate (Strecker et al. 2006; Mulch et al. 2009). This change significantly increased precipitation and erosion, shifted the sediment source westward, and increased sediment accumulation (Uba et al. 2007).

The increasing abundance of feldspar and lithics since the late Miocene (Guandacay and Emborozú formations) indicates that chemical weathering related to an intensifying monsoonal climate during Guandacay and Emborozú time (Mulch et al. 2009) was more than balanced by increased transport efficiency in streams and a reduced transport distance.

TABLE 3.—*Indices of mineralogical maturity for Chaco Basin sandstones.*

Formation	Nr. of Samples	Qp/Qm-ratio	Nr. of Samples	Maturity Index
Emborozú	6	0.8	2	2
Guandacay	4	0.6	4	3
Tariquia	25	0.4	10	9
Yecua	7	0.1	7	50
Petaca	30	0.1	22	19

"Maturity Index" denotes the ratio (Qm + Qp + Qch) / (F + L).

Tectonic Implications and Temporal Evolution of Foreland Basin Development

The Chaco foreland-basin fill records the eastward migration of the deformation front and Andean uplift (Echavarria et al. 2003; Ege 2004; Barnes et al. 2008; Uba et al. 2006; Uba et al. 2009). In the Oligocene to middle Miocene, sandstone composition of the Petaca Formation along the present-day Subandean front documents the ongoing unroofing of an eastern craton source, complemented by subordinate intrabasinal erosion in a tectonically quiet cratonal setting (Gubbels et al. 1993; Uba et al. 2006; Uba et al. 2009). Concurrent thrusting and exhumation in the Eastern Cordillera during this time (e.g., Sempere et al. 1990; Kley 1996; Ege et al. 2007; Barnes et al. 2008) is not reflected in Petaca sediments or in the paleocurrent data due to the large distance of the depocenter from the Eastern Cordillera. We thus agree with Horton et al. (2002) that the Eastern Cordillera likely formed a structural barrier to sediment dispersal starting in late Oligocene because we see no petrographic indication to the contrary (especially a higher volcanic contribution, expressed in Lv and F).

During the 14 to 8 Ma interval, roughly corresponding to the time of Yecua deposition, the Interandean belt likely formed a source area for the oldest west-derived sediments to the Chaco basin (Ege et al. 2007; Barnes et al. 2008); timing and uplift rates in the region match the calculated values for foreland-basin subsidence well (Coudert et al. 1995; Echavarria et al. 2003). This trend from western sources, however, is barely expressed in Yecua sandstone composition. We interpret its dominant craton-interior provenance, slightly reduced feldspar and slightly increased lithic components as reflecting the beginning of a minor influence of a recycled-orogen source (see Qm-F-Lt-diagram of Fig. 8). Our interpretation is supported by the pronounced increase in shortening (Echavarria et al. 2003; Uba et al. 2009) and exhumation rates (Ege et al. 2007; Barnes et al. 2008) during the late Miocene, the result of low-angle basement thrusting and the arrival of the deformation front in the western Subandean Zone (e.g., Gubbels et al. 1993; Moretti et al. 1996; Kley et al. 1997; Echavarria et al. 2003; Ege 2004; Uba et al. 2009). Active thrusting is also evidenced by high subsidence rates, which resulted in increased accommodation space (Coudert et al. 1995; Uba et al. 2006). Thus, there probably were only minor contributions of western Andean sources to the basin during the late Miocene. The dominance of fine-grained sediments during the deposition of Yecua Formation indicates that subsidence outpaced sediment supply, and that not much sediment reached the study area from the orogen (Flemings and Jordan 1989).

From 8 to 3.3 Ma, orogen-sourced clastics became dominant in the Chaco Basin. This period correlates with a shift in the paleo-drainage pattern, extensive denudation, and high sediment accumulation rates in the study area (Ege 2004; Uba et al. 2007; Barnes et al. 2008). We suggest that the 14–8 Ma major thrusting episode, subsequent forward migration of the deformation front, and increased accommodation space attained their peak (large crustal load and large wavelength) shortly before the onset of Tariquia deposition.

Up to 5-km-thick Cambrian to lower Ordovician quartzose shelf sandstones of the Interandean zone were eroded between 35 and 10 Ma, were shed eastward, and likely accumulated in (now eroded) accommodation space overlying the present Subandean Zone. Much of this quartzose material likely again became mobilized in the late Miocene and formed the bulk of Tariquia and Guandacay sandstones. Tariquia and Guandacay sediments are currently being uplifted anew along the Subandean front and shed eastward. This recycling of Andean material is contemporaneous with the migration of the foredeep depozone into the study area caused by the onset of deformation in the western Subandean zone (Ege et al. 2007; Barnes et al. 2008; Uba et al. 2009).

The Pliocene and younger Emborozú Formation (3.3 Ma to present) marks the period of major thrusting in the Subandean belt and the arrival of the deformation front in the western Chaco basin in the Pliocene (Gubbels et al. 1993; Moretti et al. 1996; Echavarria et al. 2003; Ege 2004; Barnes et al. 2008; Uba et al. 2009). This thrusting is reflected in the dominance of high lithic and low feldspar abundance in the Emborozú sandstone, thus suggesting a major contribution by a recycled-orogen source. The (sub-) recent drainage pattern, the active seismicity, and the morphology demonstrates the present uplift, deformation, and erosion of Chaco basin fill and of Paleozoic strata, both expressed in the composition of coarse-grained sandstones and boulder-size conglomerates in the wedge-top depozone (Uba et al. 2006).

CONCLUSIONS

The sandstones of the Bolivian Chaco foreland basin record the approaching front of the Andean orogen not only texturally and sedimentologically but also through distinct petrographic changes. Sandstones of the basal Petaca Formation indicate a cratonic-interior provenance with a high degree of mineralogical maturity. Associated reworked paleosols indicate a high degree of recycling of a thin continental unit, spanning a long time period and short transport distances in an arid to semihumid climate.

Yecua Formation sandstones also indicate a cratonic-interior source but show a minor contribution by a quartzose recycled-orogen provenance. Its extensive shoreline systems were prone to sedimentary recycling. Tariquia Formation sandstones mark a pronounced change in provenance and show a high contribution from fold-and-thrust-belt source rocks, overwhelming the craton-interior provenance. These cratonic characteristics may result from the recycling of older formations of continental sedimentary petrographic character or from the exposure of Mesozoic strata in the rising Subandean Belt.

The decreasing-quartz, increasing-feldspar and increasing-lithic trends in the Tariquia, Guandacay and Emborozú formations likely record the approaching orographic front of the Andean orogen through increased stream power and progressively shorter transport distances. Because the mid-Miocene rise of the Eastern Andean Cordillera (Horton et al. 2002; Ege et al. 2007) provided an early drainage barrier, sandstones of the Chaco Basin do not contain information on Andean volcanism, thus suggesting that the Altiplano was a closed basin by this time. The changing sedimentary facies and sandstone composition suggests the formation of a climate-affecting orographic barrier between 14 and 8 Ma.

ACKNOWLEDGMENTS

This research project represents part of the first author's Ph.D. thesis and was supported by the DFG-funded SFB 267 and Chaco S.A., Santa Cruz, Bolivia. We thank Oscar Araníbar, Fernando Alegría, and Nigel Robinson of Chaco S.A. for financial and logistic assistance. M. Grundmann assisted in drafting figures. D. Mertmann and E. Scheuber are thanked for critical comments and help on an early version of the manuscript. Formal reviews by JSR reviewers Brian Hampton, Luis Fernando de Ros, and Salvatore Critelli significantly improved the manuscript.

REFERENCES

Allmendinger, R.W., Jordan, T.E., Kay, S.M., and Isacks, B.L., 1997, The Evolution of the Altiplano–Puna Region of the central Andes: Annual Review of Earth and Planetary Sciences, v. 25, p. 139–174.

Baby, P., Herail, G., Salinas, R., and Sempere, T., 1992, Geometry and kinematic evolution of passive roof duplexes deduced from cross-section balancing—example from the foreland thrust system of the southern Bolivian Subandean zone: Tectonics, v. 11, p. 523–536.

Barke, R., and Lamb, S., 2006, Late Cenozoic uplift of the Eastern Cordillera, Bolivian Andes: Earth and Planetary Science Letters, v. 249, p. 350–367.

Barnes, J.B., Ehlers, T.A., McQuarrie, N., O'sullivan, P.B., and Tawackoli, S., 2008, Thermochronometer record of the central Andean Plateau growth: Tectonics, v. 27, TC3003, doi: 10.1029/2007TC002174.

Bilodeau, W.L., and Keith, S.B., 1986, Lower Jurassic Navajo–Aztec-equivalent sandstones in southern Arizona and their paleogeographic significance: American Association of Petroleum Geologists, Bulletin, v. 70, p. 690–701.

Blatt, H., 1967, Provenance determinations and recycling of sediments: Journal of Sedimentary Petrology, v. 37, p. 1031–1040.

Coira, B., Kay, S.M., and Viramonte, J., 1993, Upper Cenozoic magmatic evolution of the Argentine Puna—A model for changing subduction geometry: International Geology Review, v. 35, p. 677–720.

Coudert, L., Frappa, M., Viguier, C., and Arias, R., 1995, Tectonic subsidence and crustal flexure in the Neogene Chaco basin of Bolivia: Tectonophysics, v. 243, p. 277–292.

Cox, R., and Lowe, D.R., 1995, A conceptual review of regional-scale controls on the composition of clastic sediment and the co-evolution of the continental blocks and their sedimentary cover: Journal of Sedimentary Research, v. 65, p. 1–12.

Critelli, S., and Ingersoll, R.V., 1995, Interpretation of neovolcanic versus palaeovolcanic sand grains: an example from Miocene deep-marine sandstone of the Topanga Group (Southern California): Sedimentology, v. 42, p. 783–804.

Critelli, S., Marsaglia, K.M., and Busby, C.J., 2002, Tectonic history of a Jurassic backarc basin sequence (the Gran Cañon Formation) based on compositional modes of tuffaceous deposits: Geological Society of America, Bulletin, v. 114, p. 515–527.

Critelli, S., Le Pera, E., Galuzzo, F., Milli, S., Moscatelli, M., Perrotta, S., and Santantonio, M., 2007, Interpreting siliciclastic–carbonate detrital modes in foreland basin systems: an example from Upper Miocene arenites of the Central Apennines, Italy, *in* Arribas, J., Critelli, S., and Johnsson, M., eds., Sedimentary Provenance: Petrographic and Geochemical Perspectives: Geological Society of America, Special Paper 420, p. 107–133.

DeCelles, P.G., and Horton, B.K., 2003, Early to middle Tertiary foreland basin development and the history of Andean crustal shortening in Bolivia: Geological Society of America, Bulletin, v. 115, p. 58–77.

Dickinson, W.R., 1970, Interpreting detrital modes of graywacke and arkose: Journal of Sedimentary Petrology, v. 40, p. 695–707.

Dickinson, W.R., 1985, Interpreting provenance relations from detrital modes of sandstones, *in* Zuffa, G.G., ed., Provenance of Arenites: Dordrecht, D. Reidel Publishing Company, p. 333–361.

Dickinson, W.R., and Suczek, C.A., 1979, Plate tectonics and sandstone compositions: American Association of Petroleum Geologists, Bulletin, v. 63, p. 2164–2182.

Dunn, J.F., Hartshorn, K.G., and Hartshorn, P.W., 1995, Structural styles and hydrocarbon potential of the Subandean thrust belt of Southern Bolivia *in* Tankard, A.J., Suárez Soruco, R., and Welsink, H.J., eds., Petroleum Basins of South America: American Association of Petroleum Geologists, Memoir 62, p. 523–543.

Echavarria, L., Hernández, R., Allmendinger, R., and Reynolds, J., 2003, Subandean thrust and fold belt of northwestern Argentina: Geometry and timing of the Andean evolution: American Association of Petroleum Geologists, Bulletin, v. 87, p. 965–985.

Ege, H., 2004, Exhumations und Hebungsgeschichte der zentralen Anden in Südbolivien (21°S) durch Spaltspur-Thermochronologie an Apatit [Ph.D. Thesis]: Freie Universität Berlin, Germany, 173 p.

Ege, H., Sobel, E.R., Scheuber, E., and Jacobshagen, V., 2007, Exhumation history of the southern Altiplano plateau (southern Bolivia) constrained by apatite fission track thermochronology: Tectonics, v. 26, TC1004, doi: 10.1029/2005TC001869.

Erdtmann, B.D., Kley, J., Müller, J., and Jacobshagen, V., 1995, Ordovician basin dynamics and new graptolite data from the Tarija region, Eastern Cordillera, south Bolivia: 7th International symposium on the Ordovician System: SEPM, Pacific Section, Fullerton, p. 69–73.

Flemings, P.B., and Jordan, T.E., 1989, A synthetic stratigraphic model of foreland basin development: Journal Geophysical Research, v. 94, p. 3851–3866.

Folk, R.L., 1951, Stages of textural maturity in sedimentary rocks: Journal of Sedimentary Petrology, v. 21, p. 127–130.

Folk, R.L., 1974, Petrology of Sedimentary Rocks: Austin, Texas, U.S.A., Hemphill, 182 p.

Gazzi, P., 1966, Le arenarie del flysch sopra cretaceo dell'Appennino modenese; correlazioni con il flysch di Monghidoro: Mineralogica et Petrographica Acta, v. 16, p. 69–97.

Gubbels, R.W., Isacks, B.L., and Farrar, E., 1993, High-level surfaces, plateau uplift, and foreland development, Bolivian central Andes: Geology, v. 21, p. 695–698.

Horton, B.K., Hampton, B.A., Lareau, B.N., and Baldellon, E., 2002, Tertiary provenance history of the northern and central Altiplano (central Andes, Bolivia): A detrital record of plateau-margin tectonics: Journal of Sedimentary Research, v. 72, p. 711–726.

Hulka, C., 2005, Sedimentary and tectonic evolution of the Cenozoic Chaco foreland basin, southern Bolivia [Ph.D. Thesis]: Freie Universität Berlin, Germany, 101 p.

Hulka, C., Gräfe, K.U., Sames, B., Uba, C., and Heubeck, C., 2006, Depositional setting of the middle to late Miocene Yecua Formation of the Chaco Foreland basin, southern Bolivia: Journal of South American Earth Science, v. 21, p. 135–150.

Ingersoll, R.V., Bullard, T., Ford, R., Grimm, J., Pickle, J., and Sares, S., 1984, The effect of grain size on detrital modes: a test of the Gazzi–Dickinson point-counting method: Journal of Sedimentary Petrology, v. 54, p. 102–116.

Jacobshagen, V., Müller, J., Wemmer, K., Ahrendt, H., and Manutsoglu, E., 2002, Hercynian deformation and metamorphism in the Cordillera Oriental of Southern Bolivia, Central Andes: Tectonophysics, v. 345, p. 119–130.

Johnsson, M.J., 1990, Tectonics versus chemical-weathering controls on the composition of fluvial sands in tropical environments: Sedimentology, v. 37, p. 713–726.

Johnsson, M.J., Stallard, R.F., and Lundberg, N., 1991, Controls on the composition of fluvial sands from a tropical weathering environment: Sands of the Orinoco River drainage basin, Venezuela and Colombia: Journal of Geology, v. 96, p. 263–277.

Jones, J., 1985, The southern border of the Guaporé Shield in western Brazil and Bolivia: An interpretation of its geologic evolution: Precambrian Research, v. 85, p. 111–135.

Jordan, T.E., Reynolds, J.H., and Erikson, J.P., 1997, Variability in age of initial shortening and uplift in the central Andes, 16–33°30′S, *in* Ruddiman, W.F., ed., Tectonic Uplift and Climate Change: New York, Plenum Press, p. 41–61.

Kley, J., 1993, Der Übergang vom Subandin zur Ostkordillere in Südbolivien (21°15–22° S): Geologische Struktur und Kinematik: Berliner Geowissenschaftliche Abhandlungen, v. 156, p. 1–88.

Kley, J., 1996, Transition from basement-involved to thin-skinned thrusting in the Cordillera Oriental of southern Bolivia: Tectonics, v. 15, p. 763–775.

Kley, J., and Reinhardt, M., 1994, Geothermal and tectonic evolution of the eastern Cordillera and the Subandean Ranges of southern Bolivia, *in* Reutter, K.J., Scheuber, E., and Wigger, P., eds., Tectonics of the South Central Andes: Berlin, Springer Verlag, p. 155–170.

Kley, J., Müller, J., Tawackoli, S., Jacobshagen, V., and Manutsoglu, E., 1997, Pre-Andean and Andean-age deformation in the Eastern Cordillera of southern Bolivia: Journal of South American Earth Sciences, v. 10, p. 1–19.

Mack, G.H., 1984, Exceptions to the relationship between plate tectonics and sandstone composition: Journal of Sedimentary Petrology, v. 54, p. 212–220.

Marshall, L.G., and Sempere, T., 1991, The Eocene to Pleistocene vertebrates of Bolivia and their stratigraphic context: A review, *in* Suárez Soruco, R., ed., Fosiles y Facies de Bolivia: Revista Técnica de Yacimientos Petrolíferos Fiscales Bolivianos, v. 1, p. 31–652.

Marshall, L.G., Sempere, T., and Gayet, M., 1993, The Petaca (late Oligocene–middle Miocene) and Yecua (late Miocene) formations of the Subandean Chaco basin, Bolivia and their tectonic significances: Laboratoire de Geologie de Lyon, Documents, v. 125, p. 291–301.

Molnar, P., and England, P., 1990, Late Cenozoic uplift of mountain ranges and global climate change—chicken or egg: Nature, v. 346, p. 29–34.

Moretti, I., Baby, P., Mendez, E., and Zubieta, D., 1996, Hydrocarbon generation in relation to thrusting in the Sub Andean Zone from 18° to 22°S, Bolivia: Petroleum Geoscience, v. 2, p. 17–28.

Mulch, A., Uba, C.E., Strecker, M., Schönberg, R., and Chamberlain, C.P., 2009, A Late Miocene stable isotope paleosoil record of Andean foreland precipitation: Geochimica et Cosmochimica Acta, v. 73, Supplement 1, A914 p.

Müller, J., Kley, J., and Jacobshagen, V., 2002, Structure and Cenozoic kinematics of the eastern Cordillera, southern Bolivia (21°S): Tectonics, v. 21, p. 1–23.

Pettijohn, F.J., 1975. Sedimentary Rocks: New York, Harper and Row, 628 p.

Sempere, T., Hérail, G., Oller, J., and Bonhomme, M.G., 1990, Late Oligocene–early Miocene major tectonic crisis and related basins in Bolivia: Geology, v. 18, p. 946–949.

Strecker, M.R., Mulch, A., Uba, C.E., Schmitt, A.K., and Chamberlain, C., 2006, Late Miocene onset of the South American Monsoon: EOS, Transactions, American Geophysical Union, v. 87, p. T31E–06.

Suárez Soruco, R., 2000, Geological Compendium of Bolivia: Revista Técnica de Yacimientos Petrolíferos Fiscales Bolivianos, 18 (part A), p. 1–76.

Suttner, L.J., and Basu, A., 1981, Climate and the origin of quartz arenites: Journal of Sedimentary Petrology, v. 51, p. 1235–1246.

Uba, C.E., Heubeck, C., and Hulka, C., 2005, Facies analysis and basin architecture of the Neogene Subandean synorogenic wedge, southern Bolivia: Sedimentary Geology, v. 180, p. 91–123.

Uba, C.E., Heubeck, C., and Hulka, C., 2006, Evolution of the late Cenozoic Chaco foreland basin, Southern Bolivia: Basin Research, v. 18, p. 145–170.

Uba, C.E., Strecker, M., and Schmitt, A.K., 2007, Increased sediment accumulation rates in the Central Andes during the late Miocene due to climate forcing: Geology, v. 35, p. 979–982.

Uba, C.E., Kley, J., Strecker, M., and Schmitt, A., 2009, Unsteady evolution of the Bolivian Subandean thrust belt: the role of enhanced erosion and clastic wedge progradation: Earth and Planetary Science Letters, v. 281, p. 134–146.

Whipple, K.X., and Meade, B.J., 2006, Orogen response to changes in climatic and tectonic forcing: Earth and Planetary Science Letters, v. 243, p. 218–228.

Willett, S.D., 1999, Orogeny and orography: the effects of erosion on the structure of mountain belts: Journal of Geophysical Research, v. 104, p. 28,957–28,965.

Zuffa, G.G., 1980, Hybrid arenites: their composition and classification: Journal of Sedimentary Petrology, v. 50, p. 21–27.

Received 8 March 2009; accepted 7 October 2009.